J Appl Electrochem (2010) 40:257–263
DOI 10.1007/s10800-009-9999-7

ORIGINAL PAPER

Electrodeposited platinum catalysts over hierarchical carbon monolithic support

Mariano M. Bruno · Esteban A. Franceschini · Gabriel A. Planes · Horacio R. Corti

Received: 22 April 2009 / Accepted: 16 August 2009 / Published online: 28 August 2009

Abstract Mesoporous deposits of platinum catalysts were electrodeposited over monolith carbon with hierarchical porous structure. The liquid crystal used as a template allowed the electrodeposition of the catalyst on the outer region of the carbon with low penetration in the porous structure. The platinum hexagonal mesostructured deposits exhibits an excellent stability enhanced by the roughness of the carbon support. The mass activity for the electrooxidation of methanol of the mesoporous Pt catalyst supported on the hierarchical carbon is similar to that observed on gold and to that reported for commercial Pt nanoparticulated catalysts, even when this catalyst has a smaller Pt load than the commercial one. Also, the poisoning rate of the mesoporous catalyst is lower than that observed for the commercial catalyst. The integrated system of structured materials could be suitable for the fabrication of modified electrodes in small scale applications.

Keywords Platinum · Mesoporous catalyst · Hierarchical carbon · Methanol oxidation · Poisoning rate

Abbreviations

PEM	Polymer exchange membrane
HC	Hierarchical carbon
RF	Resorcinol formaldehyde
MC	Mesopororous catalyst
HCMC	Hierarchical carbon–mesopororous catalyst
ca.	Circa
RHE	Reversible hydrogen electrode
δ	Poisoning rate
RMS	Root mean square

M. M. Bruno · E. A. Franceschini · H. R. Corti (✉)
Grupo de Celdas de Combustible, Departamento de Física de la Materia Condensada, Centro Atómico Constituyentes, CNEA
Av. General Paz 1499 (1650), San Martín, Buenos Aires, Argentina
e-mail: hrcorti@cnea.gov.ar

G. A. Planes
Departamento de Química, Facultad de Ciencias Exactas, Fisicoquímicas y Naturales, Universidad Nacional de Río Cuarto, Agencia Postal No 3, 5800 Río Cuarto, Argentina

1 Introduction

Nanostructured materials are good candidates for innovative applications in fuel cells [1], supercapacitors [2], electrochemical sensors [3], and other electrochemical devices. In the last two decades several methods of production of structured materials were proposed, leading to a wide range of materials with tailored composition, structure and properties (selected redox reactions, mass transport management, increased electroactive area), as recently reviewed [4, 5].

Several devices employed to generate, and store energy or energy vectors, like hydrogen, are ground on electrochemical reactions [2, 3, 6–10]. The efficiency of an electrochemical process could be strongly affected by the accessibility of the gaseous or liquid reactants to the catalysts surface, the release of the products of the reaction, or the blocking of the catalyst electroactive area. Therefore, their performance could be improved beyond the intrinsic properties of the used materials by a suitable design and integration of the different components of the device. In the case of a fuel cell these components include the gas diffusion layer, the catalyst support and the catalysts itself.

Metals such as nickel, platinum, iridium, rhodium, etc. and its alloys are capable of catalyst a wide variety of

electrochemical reactions [6–14], including the electrooxidation of methanol or ethanol in direct alcohol PEM fuel cells and reforming of small molecules, like methane, to generate hydrogen employing nickel and rhodium based catalysts.

Recent studies propose the use of mesoporous electrocatalyst layer formed by electrodeposition [15, 16]. Mesoporous platinum deposited on gold has shown better performance than Pt catalysts supported on commercial carbon, compared at similar Pt load [16].

In this study, the mesoporous platinum catalyst, electrodeposited over hierarchical carbon and gold from precursors dissolved in the aqueous domains of a lyotropic liquid crystalline phase, were analyzed separately. The use of a viscous lyotropic liquid is expected to assure the electrodeposition of the catalyst only on the outer region of the carbon support, allowing the integration of the catalyst with the structured monolithic carbon, which act as gas diffusion layer and current collector [17, 18]. This preparation procedure would improve the electric contact between the catalysts and the gas diffusion layer, while the tuneable porosity of the carbon could provide suitable ways for the outlet of the gaseous carbon dioxide [19] generated during the methanol electrooxidation.

Here, we report the study of mesoporous platinum electrodeposited directly over a monolithic carbon with hierarchical pore distribution, which could have a synergic effect on the electrooxidation process through a suitable management of mass transport from/to the catalyst region [20, 21]. The monolithic carbon used in this study is formed by porous (nanometer size) spheres, whose packing generates mesopores, and straight capillaries crossing the bulk material.

The mesoporous platinum electrode over a hierarchical carbon monolith was studied for the electrooxidation of methanol because it could be a promising electrocatalyst system in direct methanol PEM fuel cells [22–25].

The studies of binary catalyst electrodeposition, wearing down and durability of this new type of integrated materials, as well as their integration and characterization in fuel cell, and other energy devices will be carried out in a forthcoming study.

2 Experimental part

2.1 Materials

2.1.1 Hierarchical porous carbon

The Hierarchical Carbon (HC) containing mesopores and capillaries was obtained using the method described elsewhere [26]. Briefly, it uses a polyelectrolyte (polydilayldimethylammonium chloride, PDADMAC, Sigma-Aldrich) as a structuring agent for mesopores in a resorcinol (Sigma-Aldrich) formaldehyde (Cicarelli) polymer precursor of carbon, and a commercial polypropylene fiber, as a hard template for generation of the capillaries. The resulting cubic shaped monolithic resorcinol–formaldehyde polymer–polypropylene composite was dried in air for several days and carbonized under nitrogen at 800 °C with a heating rate of 40 K h^{-1}. A typical monolithic carbon sample has an area of 5 cm^2, a thickness of 300 μm, and capillaries of diameter around 15 μm, connecting both sides of the support, as observed from the Scanning Electron Microscopy (SEM) image of a transversal cut of the monolithic carbon shown in Fig. 1a. As mentioned before, the surface density of capillaries can be easily controlled by adjusting the amount of the polypropylene template. In Fig. 1b, the morphology of the surface carbon formed by spherical particles of ca. 60 nm can be observed. According to previous study [27, 28], the packing of these particles forms the mesoporous structure. However, the high BET surface area of this material

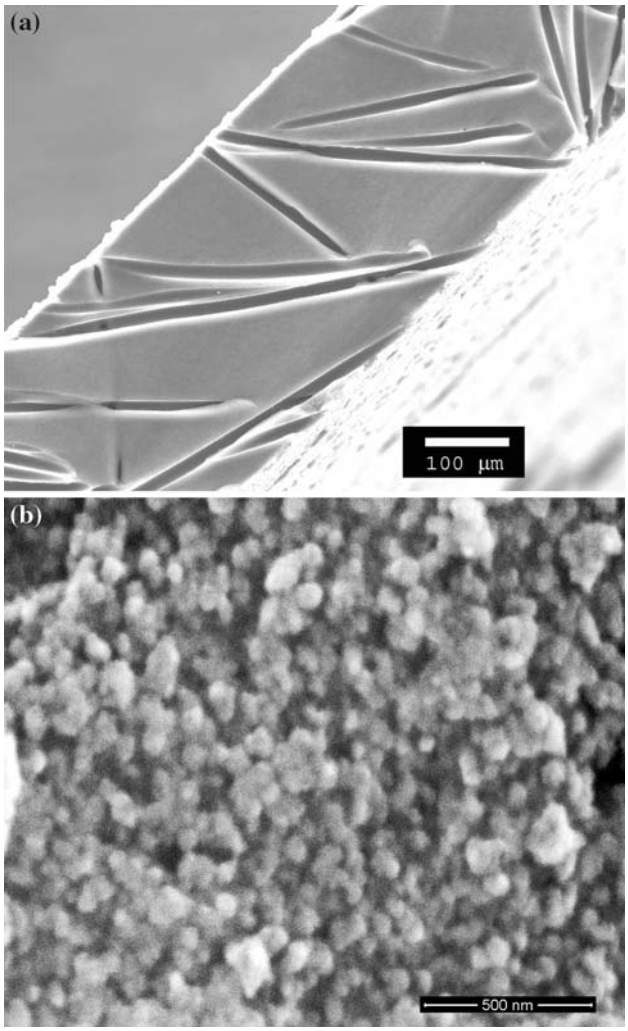

Fig. 1 SEM image of hierarchical carbon: (**a**) transversal cut; (**b**) surface top view

(749 m^2 g^{-1}) could not be accounted by the surface of the 60 nm globular particles, which only contributes with about 70 m^2 g^{-1}. It was estimated by molecular simulation [27] that the globular forms observed in Fig. 1b are clusters of small carbon nanoparticles (5–15 nm). The Barret, Joyner and Halenda (BJH) model of pore size distribution analysis [29] shows a peak around 40 nm and it is coherent with a carbon porous structure having mesopores.

A high surface roughness of the carbon is observed, which is essential for anchoring the catalyst layer during the electrodeposition, as we will discuss below.

2.1.2 *Mesoporous platinum*

Silica chips, covered with a thin film of gold (EMF, Evaporated Metal Film Corporation), and hierarchical carbon were used as supports for the electrodeposition. The mesoporous catalyst (MC) was obtained by electrochemical reduction of a mixture of a 8 wt% aqueous solution of hexachloroplatinic acid (Aldrich) and a 50 wt% aqueous solution of octaethyleneglycol monohexadecyl ether ($C_{16}EO_8$) (Brij 56®, Aldrich), following the method proposed by Planes et al. [16]. This method of electrochemical reduction of metallic salts dissolved in the aqueous domains of a liquid crystal solution was a modification of the procedure by Attard et al. [30]. In this case, a lower initial concentration of precursor was used [16].

The mass of Pt electrodeposited by unit area, estimated by assuming a faradic efficiency of 75% for Pt^{+4} reduction [31], corresponds to 0.093 mg Pt cm^{-2} on gold and 0.168 mg Pt cm^{-2} on carbon, respectively. However, it should be noted that this calculation overestimates the mass deposited on carbon because the double layer current is significantly major than in the case of gold.

The thickness of the mesoporous platinum layer would be about 35 nm on gold and 63 nm on carbon if it would be deposited as a uniform layer on the surface, but these figures should be taken just as a rough estimation because the layer is certainly uneven.

Residual compounds after the electrodeposition were removed from the Hierarchical Carbon–Mesoporous Catalyst (HCMC) system by successive washes with water during 72 h.

2.2 Characterization

2.2.1 *Morphology and structure*

Scanning electron microscope images were taken with a Quanta 200 (FEI Company).

The AFM (Nanoscope IIIa, Veeco) images of the carbon were acquired using the contact mode. A commercial Si tip having an anisotropic shape was used, with the nominal radius <10 nm, and a nominal spring constant of 40 N m^{-1} (36.50 N m^{-1} measured) (MPP-11200, Veeco Probes).

The samples roughness were characterized through the Root Mean Square (RMS), that is, the standard deviation of the coordinate Z, perpendicular to the surface plane, over a given area, defined by the equation:

$$\mathrm{RMS} = \left(\frac{\sum_{i=1}^{N} (Z_i - Z_{\mathrm{av}})^2}{N} \right)^{1/2} \quad (1)$$

where Z_{av} is the average value, Z_i is the current position of the piezo when the tip contact the sample, and N is the number of points within the analysed area.

Glancing incidence small angle X-ray scattering (GI-SAXS) is a technique widely used to determine the structure of ordered porous materials. It was carried out in the SAXS1 line of the National Synchrotron Light Laboratory (LNLS, Campinas–Brazil) using an incident angle of 1.5°.

2.2.2 *Electrochemical*

The electrochemical performance of the materials was analyzed with a thermostatized cell of three electrodes configuration. A platinum electrode and a Reversible Hydrogen Electrode (RHE) were used as counter and reference electrode. Cyclic voltammetry and chronoamperometry techniques were performed with a potentiostat (TEQ_02) with a microcontroller, connected via an RS232 interface, was used for the electrochemical characterization.

3 Results and discussion

3.1 Hierarchical carbon

As discussed in Sect. 2.1 and shown in Fig. 1a, b, the monolithic carbon has a hierarchical pore structure composed by nanopores and capillaries, which would improve the mass transport from or to the catalytic region when the catalysts are deposited on it. For instance, in the case of a direct methanol fuel cell the monolithic carbon can act as gas diffusion layer and catalyst support, while the capillaries would facilitate the outlet of carbon dioxide produced in the anode.

The electrochemical characterization of the hierarchical carbon was realized in 1 M H_2SO_4. The current response, shown in Fig. 2, was expressed as specific capacitance. The capacitance of the material, 200 F g^{-1}, was obtained by integrating the stored charge stored over all the potential range. The high capacitance obtained in the acid medium is due to the contribution of the double layer and electroactive groups (pseudocapacitance). The broad band observed around 650 mV is assigned to redox reaction of the superficial quinone groups. These oxygenated groups (acidic, basic, and neutrals) affect the capacitance, because some of

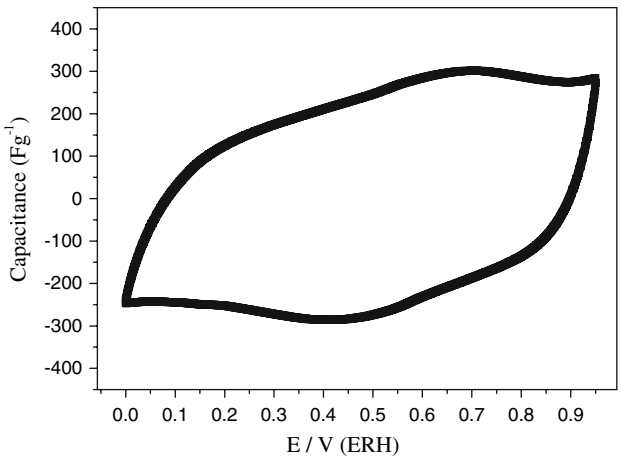

Fig. 2 Voltamperogramm of hierarchical carbon in 1 M H_2SO_4. Scan rate: 1 mV seg^{-1}

them are electroactive to faradaic charge (quinone groups) and, at the same time, all of them improve the wettability of the material [32]. For carbon materials obtained with similar procedures, the contribution of this pseudocapacitance to the total capacitance were reported to be ca. 50 % [33, 34]. Furthermore, it is possible to assess the accessible area of the material by assuming a double layer capacitance of 0.20 F m^{-2}, typical of carbon materials [35]. Thus, a double layer contribution of 100 F g^{-1} in our hierarchical carbon represents an electroactive surface area of 500 m^2 g^{-1}. In comparison with the 749 m^2 g^{-1} obtained by N_2 isotherms adsorption, it would indicate good accessibility to almost all surface area of the material [36].

3.2 Mesoporous catalyst characterization

The structure of the mesoporous platinum electrodeposited over gold [37, 38], (as determined through the GISAXS pattern shown in Fig. 3), is compatible with a 2D hexagonal (p6mm) mesostructure, oriented with a [01] plane parallel to the surface with a typical interpore distance of 6 nm, that is, the expected behavior considering the liquid crystal structure and the phase diagram of Brij 56 [39–41] under the conditions of temperature and concentration employed in the catalyst deposition.

The chronoamperometry response of the mesoporous platinum film on gold, shown in Fig. 4b was measured at 25 °C in 1 M CH_3OH/0.5 M H_2SO_4 solution, with a step from 450 mV (open circuit potential) to 800 mV vs. RHE and a duration of 20 min, as normally used in poisoning rate tests [42, 43]. The rapid current decrease at short times could be attributed to blocking of the catalyst surface [31]. The rate of current decay becomes exponential at longer time and a limit current density of 1.9 mA cm^{-2} is reached, considering the geometrical area of the electrode.

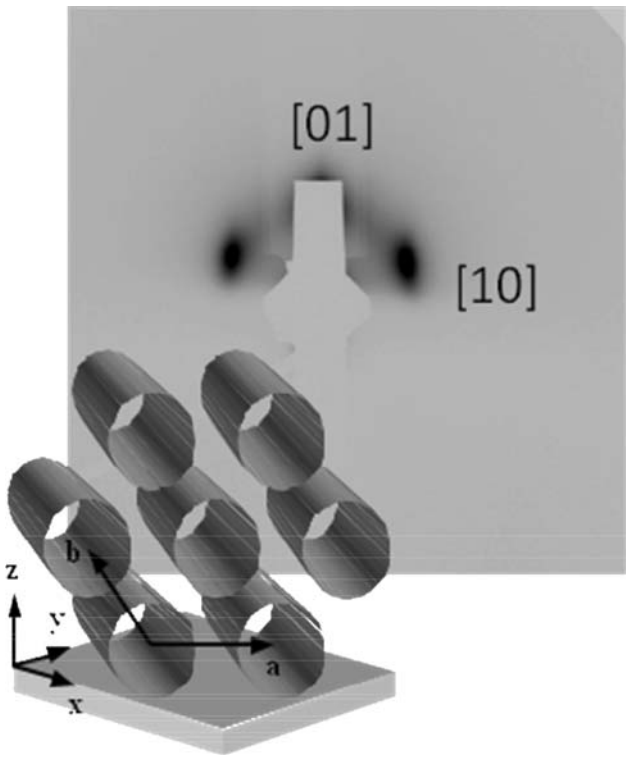

Fig. 3 GISAXS patterns of the deposited platinum thin films templated with Brij 56® and schematic draw of p6mm mesostructure

3.3 HCMC characterization

The electrochemical response of the integrated HCMC system was analyzed in 1 M H_2SO_4 and 1 M CH_3OH/1 M H_2SO_4 solutions. A cyclic voltammetry was performed on the HCMC in 1 M H_2SO_4 to remove the secondary reaction products and adsorbed template. Then, a cyclic voltammetry in 1 M CH_3OH/1 M H_2SO_4 solution allowed us to obtain the range of oxidation potentials for methanol (Fig. 4a). In Fig. 4b the chronoamperometry responses with a potential step from 400 to 800 mV (the onset potential for methanol oxidation) vs. RHE in both electrolytic media are shown. The high RC (time response) characteristic of this kind of carbon could cause the shift [44] in the potential onset of methanol oxidation, commonly located close to 550 mV vs. RHE [45].

Different processes, such as catalyst oxidation, oxidation of superficial groups, and double layer charge, are involved in the relatively long time of current decay to zero observed in Fig. 4b in 1 M H_2SO_4. In the case of 1 M CH_3OH/1 M H_2SO_4 electrolytic solution, it can be seen that at short time, there is a reduction of current peak. It could be attributed to oxidation products which partially cover the catalytic layer [31]. At long time, the methanol oxidation produces a quasi-stationary current density of ca. 2.5 mA cm^{-2}.

The corresponding mass activity, that is, the current per gram of Pt, are 20 and 15 A g^{-1} on gold and hierarchical

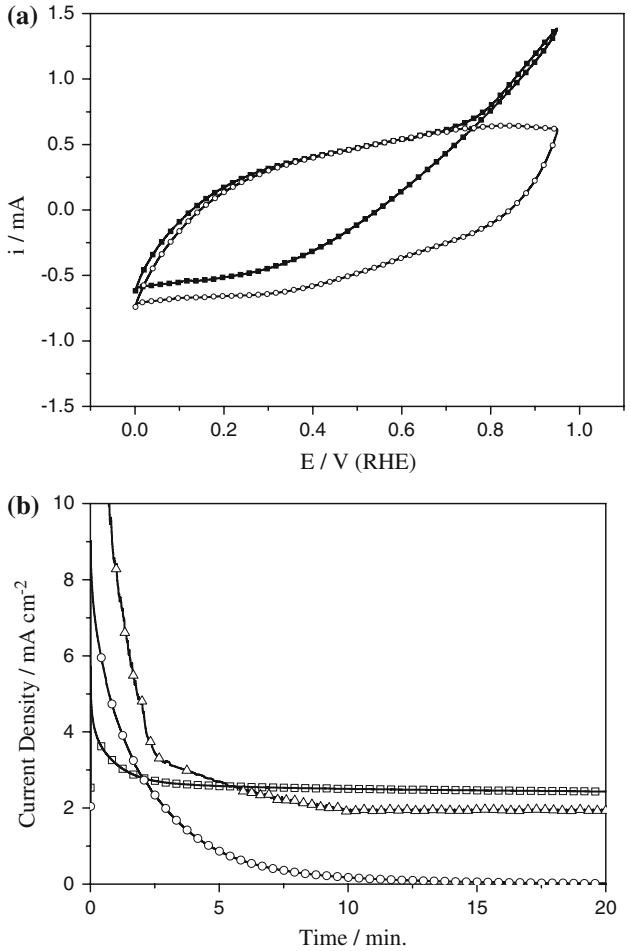

Fig. 4 **a** Voltamperogramm of hierarchical carbon–catalyst in 1 M H_2SO_4 (*open circle*) and 1 M CH_3OH/1 M H_2SO_4 (*filled square*). **b** Chronoamperometry profiles of: HCMC in 1 M H_2SO_4 (*open circle*), and in 1 M CH_3OH/1 M H_2SO_4 (*open square*), and of a thin film of MP Pt (over gold) in 1 M CH_3OH/0.5 M H_2SO_4 (*open triangle*). Scan rate: 1 mV seg^{-1}

carbon, respectively, for times of the order of several minutes. It is observed in Fig. 4b that at short times the current decay of the catalysts supported on gold is larger than that on hierarchical carbon, but both current density profiles decay linearly at longer times. Thus, the long-term poisoning rate, δ, for the mesoporous catalyst can be calculated, using the following equation [42, 46]:

$$\delta = \frac{100}{i_0}\left(\frac{\mathrm{d}i}{\mathrm{d}t}\right) \tag{2}$$

where i_o is the current extrapolated at the start of polarization, and the slope, di/dt, is evaluated from the linear decay at $t > 10$ min. The result, $\delta = 0.004\ s^{-1}$, obtained for the mesoporous catalyst on carbon (HCMC) is similar to that observed on gold, but it is lower than that reported

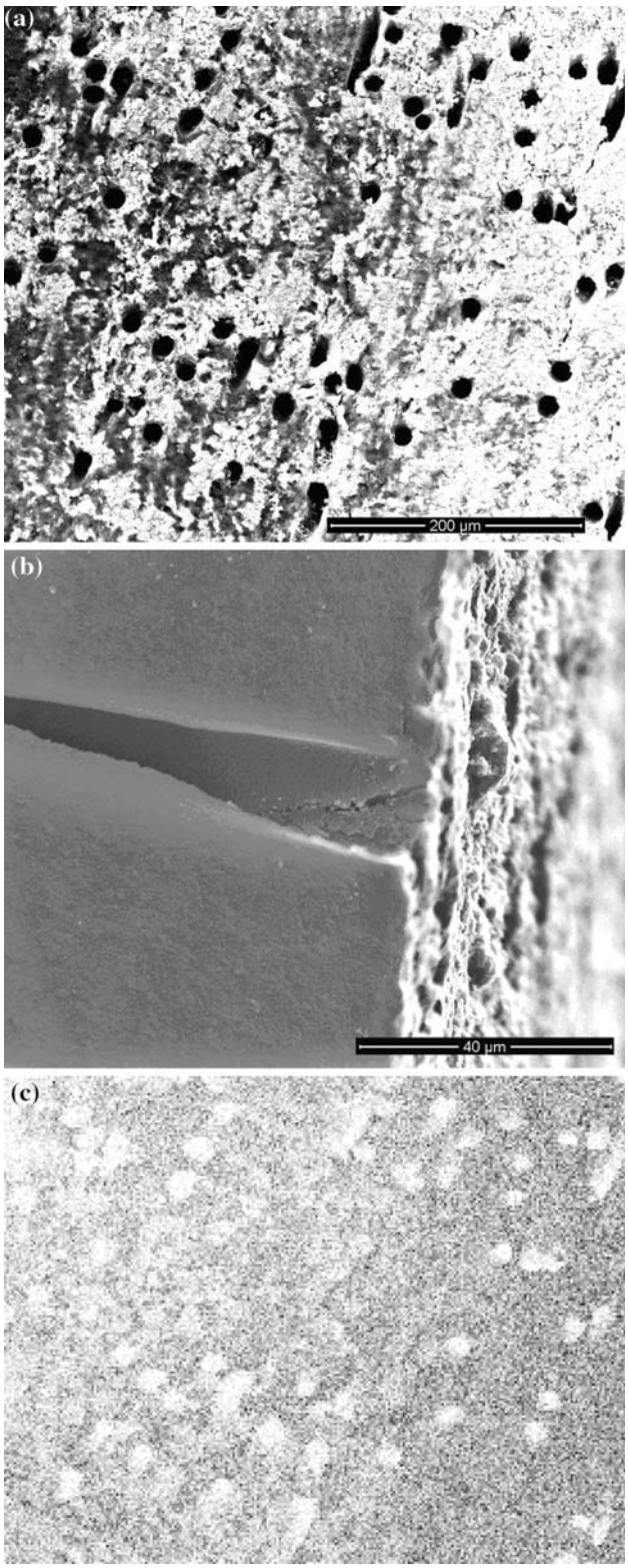

Fig. 5 **a** Image of platinum (*white area*) electrodeposited over carbon (*black area*). **b** Image of a carbon open capillary. **c** EDX mapping a surface area of 500 × 450 µm

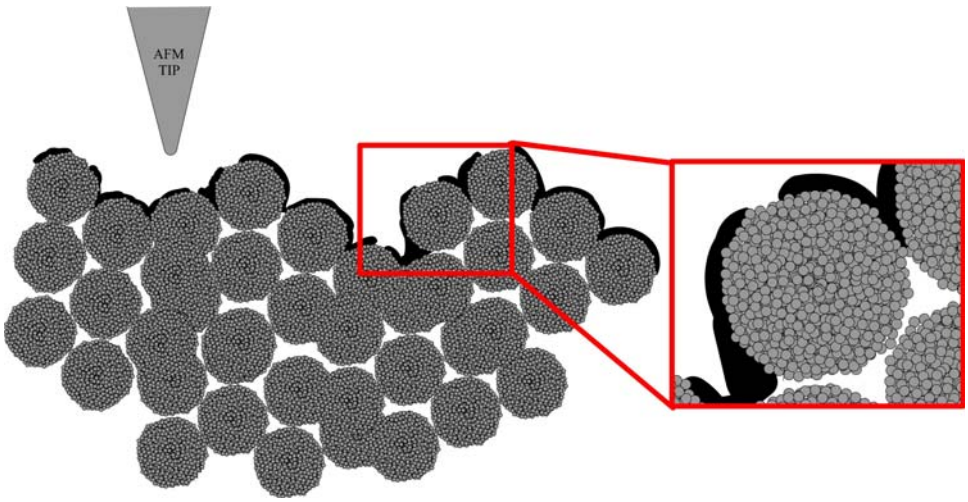

Fig. 6 Scheme of the nanoporous structure of the monolithic carbon showing the mesoporous Pt catalyst anchored in the mesoporous, and the roughness sensed by the AFM tip. Zoom: clusters of carbon nanoparticles forming larger particles (≈60 nm)

for the commercial Pt catalyst (E-TEK) by Teng et al. [47] (δ = 0.0067 s^{-1}).

The morphology of the HCMC was analyzed after the electrochemical characterization. The SEM images (Fig. 5a) show the surface of carbon coated with the electrodeposited platinum. The white regions, due to the high conductivity of platinum to the electrons, indicate the presence of the catalyst, while the dark regions correspond to both, the open capillaries and the small areas where the catalyst is absent. On the other hand, the SEM image shown in Fig. 5b confirms that the capillaries remain open, although we can not assure that the catalyst has not been deposited inside the walls of the capillaries.

It seems that the high viscosity of the precursor solution, containing Brij 56®, prevents the penetration of the catalyst precursor inside of capillaries [48].

Figure 5c shows the Energy Dispersive X-ray (EDX) mapping of platinum atoms over a surface area of 500 × 450 μm, where a homogeneously distribution of catalyst, without capping of capillaries can be observed.

Similar conditions of electrodeposition were employed over compact glassy carbon. In this case, the mesoporous Pt layer came off from the carbon support when it was electrochemically analyzed. The poor adherence of films and nanoparticles on carbon surfaces has been already reported in the literature [49, 50]. It is obvious that the generation of surface groups on carbon plays an important role in enhancing the stability of the HCMC system, although it is not clear the mechanism of these groups as anchoring sites for supported catalysts and whether this is the only factor which determines its excellent stability [51]. Additionally, the roughness caused by the mesoporosity of the surface, provides good physical anchoring sites for the electrodeposited catalyst layer [52].

AFM images, not shown here, were taken in order to analyze changes in the roughness due to the electrodeposition of mesoporous platinum. The RMS values obtained from these images are 202 and 204 nm for hierarchical carbon (before the catalyst electrodeposition) and HCMC, respectively. The results could be explained having into account the size of the porous carbon spheres [28] (around 60 nm) and the curvature radius of the AFM tip (∼10 nm), as schematically shown in the Fig. 6. The roughness of the support material is due to clustering of these porous carbon spheres (see Fig. 1b), which provide anchoring sites for the electrodeposited platinum. Therefore, the AFM tip senses the carbon surface roughness which is only slightly influenced by the platinum. The nanoporous structure of the monolithic carbon, making the major contribution to the high surface surface, is also shown in Fig. 6 where we emphasize that the deposited mesoporous Pt does not penetrate the micropores, which remain available for mass transport.

4 Conclusions

Mesoporous Pt catalysts layers were prepared on gold and hierarchical porous carbon using a surfactant (Brij 56®) template. The mesoporous structure of the carbon support provides anchoring sites to the mesostructured Pt catalyst, leading to an excellent stability. The Pt mesostructure is 2D hexagonal with an interpore distance of 6 nm. The Pt loading used in this work (ca. 0.10 mg Pt cm^{-2}) is much lower than that employed in catalysts for direct methanol fuel cells that, usually, is between 2 and 4 mg Pt cm^{-2} [53–56], although loading as low as 0.4 mg Pt cm^{-2} have bee reported for optimized catalysts [57, 58]. These results demonstrate that the integrated systems maximize the utilization of the catalysts.

The mass activity for the methanol oxidation determined at 25 °C, is of the order of 15–20 A g^{-1}, slightly lower than that previously determined for mesoporous Pt catalyst on gold prepared by the same method [10] and for a commercial catalyst of Pt nanoparticles supported on

carbon, although the poisoning rate of the last is much higher than that observed for the mesostructured Pt catalysts.

As expected, the RMS of hierarchical carbon and HCMC show similar values, indicating that the catalyst layer does not modify the roughness of the carbon support, while the deposition of Pt on the micron-sized capillaries is negligible.

In summary, we probed that is possible to deposit mesoporous Pt on a monolithic carbon whose porosity can be tuned. This HCMC system is a promising gas diffusion layer/catalyst support integrated device which could contribute to the miniaturization of direct methanol mini fuel cell for portable applications.

Acknowledgments The authors thank financial support from Agencia Nacional de Promoción Científica y Tecnológica (PICT Start Up 35403), and CONICET (PIP 5977). The contributions of Dr. G. Soler Illia and the National Synchrotron Light Laboratory (LNLS, Campinas – Brazil) in the GISAXS measurement are gratefully acknowledged. GAP and HRC are permanent research fellows of CONICET. MB and EF thank to CONICET for their fellowships.

References

1. Larminie J, Dicks A (2003) Fuel cell system explained, 2nd edn. Wiley, Chichester, New York
2. Pandolfo AG, Hollenkamp AF (2006) J Power Sources 157:11
3. Walcarius A, Sibottier E, Etienne M, Ghanbaja J (2007) Nat Mater 6:602
4. Meng Y, Gu D, Zhang F, Shi Y, Cheng L, Feng D, Wu Z, Chen Z, Wan Y, Stein A, Zhao D (2006) Chem Mater 18:4447
5. Wan Y, Shi Y, Zhao D (2008) Chem Mater 20:932
6. Kobayashi N, Takahashi S (2007) European Patent Application, Pat. N: EP1862217
7. Wang HM (2008) J Power Sources 177:506
8. Abu-Jrai A, Tsolakis A, Megaritis A (2007) Int J Hydrog Energy 32:65
9. Iojoiu EE, Domine ME, Davidian T, Guilhaume N, Mirodatos C (2007) Appl Catal A 323:147
10. Zhang B, Cai W, Li Y, Xu Y, Shen W (2008) Int J Hydrog Energy 33:4377
11. Abdelkareem MA, Nakagawa N (2006) J Power Sources 162:114
12. Haile SM (2003) Acta Mater 51:5981
13. Kulikovsky A, Kucernak A, Kornyshev AA (2005) Electrochim Acta 50:1323–1333
14. Zhang J, Yin G-P, Lai Q-Z, Wang Z-B, Cai K-D, Liu P (2007) J Power Sources 168:453
15. Cheng T, Gyenge EL (2006) Electrochim Acta 51:3904
16. Planes GA, García G, Pastor E (2007) Electrochem Commun 9:839
17. Glora M, Wiener M, Petricevic R, Probstle H, Fricke J (2001) J Non-Cryst Solids 285:283
18. Du H, Li B, Kang F, Fu R, Zeng Y (2007) Carbon 45:429
19. Meng DD, Cubaud T, Ho C-M, Kim C-J (2007) JMEMS 16:1403
20. Cheng TT, Gyenge EL (2008) J Appl Electrochem 38:51
21. Wang D-W, Li F, Liu M, Lu GQ, Cheng H-M (2007) Angew Chem Int Ed 47:373
22. Antolini E, Salgado JRC, Gonzalez ER (2006) Appl Catal B 63:137
23. Hampson NA, Willars MJ (1979) J Power Sources 4:191
24. Kirillov SA, Tsiakaras PE, Romanova IV (2003) J Mol Struct 651:365
25. Duarte MME, Pilla AS, Sieben JM, Mayer CE (2006) Electrochem Commun 8:159
26. Bruno MM, Corti HR, Barbero CA (2009) Funct Mat Lett (in press)
27. Gavalda S, Gubbins KE, Hanzawa Y, Kaneko K, Thomson KT (2002) Langmuir 18:2141
28. Yamamoto T, Mukai SR, Endo A, Nakaiwa M, Tamon H (2003) J Colloid Interface Sci 264:532
29. Rouquerol J, Avnir D, Fairbridge CW, Everett DH, Haynes JH, Pernicone N, Ramsay JDF, Sing KSW, Unger KK (1994) Pure Appl Chem 66:1739
30. Attard GS, Bartlett PN, Coleman NRB, Elliott JM, Owen JR, Wang JH (1997) Science 278:838
31. Jiang J, Kucernak A (2002) J Electroanal Chem 533:153
32. Lozano-Castelló D, Cazorla-Amorós D, Linares-Solano A, Shiraishi S, Kurihara H, Oya A (2003) Carbon 41:1765
33. Bruno MM, Cotella NG, Miras MC, Barbero CA (2005) Chem Commun 5896
34. Bruno MM (2007) Thesis, Universidad Nacional de Río Cuarto, Argentina
35. Barbieri O, Hahn M, Herzog A, Koetz R (2005) Carbon 43:1303
36. Frackowiak E, Béguin F (2001) Carbon 39:937
37. Attard GS, Bartlett PN, Coleman NRB, Elliott JM, Owen JR (1998) Langmuir 14:7340
38. Barlett PN, Gollas B, Guerin S, Marwan J (2002) Phys Chem Chem Phys 4:3835
39. Mitchell DJ (1983) J Chem Soc Faraday Trans 1:975
40. Crepaldi EL, Soler-Illia GJAA, Grosso D, Cagnol F, Ribot F, Sánchez C (2003) J Am Chem Soc 125:9770
41. Eggiman BW, Tate MP, Hillhouse HW (2006) Chem Mater 18:723
42. Jiang J, Kucernak A (2002) J Electroanal Chem 520:64
43. Jiang J, Kucernak A (2003) J Electroanal Chem 543:187
44. Conway BE (1999) Electrochemical supercapacitors: scientific fundamentals and technological applications. Kluwer Academic/Plenum Publishing, New York
45. Lim D-H, Lee W-D, Choi D-H, Park D-R, Lee H-I (2008) J Power Sources 185:159
46. Guo JW, Zhao TS, Prabhuram J, Chen R, Wong CM (2005) Electrochim Acta 51:754
47. Teng Z-H, Wang G, Wu B, Gao Y (2007) J Power Sources 164:105
48. Bender F, Chilcott TC, Coster HGL, Hibbert DB, Gooding JJ (2007) Electrochim Acta 52:2640
49. Etienne M, Walcarius A (2005) Electrochem Comm 7:1449
50. Rodríguez-Reinoso F (1998) Carbon 36:59
51. Fraga MA, Jordão E, Mendes MJ, Freitas MMA, Faria JL, Figueiredo JL (2002) J Catal 209:355
52. Seidel YE, Lindström RW, Jusys Z, Gustavsson M, Hanarp P, Kasemo B, Minkow A, Fecht HJ, Behm RJ (2008) J Electrochem Soc 155:K50
53. Cheng X, Peng C, You M, Liu L, Zhang Y, Fan Q (2006) Electrochim Acta 51:4620
54. Guo JW, Xie XF, Wang JH, Shang YM (2006) Electrochim Acta 53:3056
55. Guo J, Sun G, Wang Q, Wang G, Zhou Z, Tang S, Jiang L, Zhou B, Xin Q (2006) Carbon 44:152
56. Faghri A, Guo Z (2008) Appl Therm Eng 28:1614
57. Kim SH, Cha HY, Miesse CM, Jang JH, Oh YS, Cha SW (2009) Int J Hydrog Energy 34:459
58. Silva VS, Ruffmann B, Vetter S, Mendes A, Madeira LM, Nunes SP (2005) Catal Today 104:205